



# The paleomagnetic record at IODP Site U1307 back to 2.2 Ma (Eirik Drift, off south Greenland)



A. Mazaud<sup>a,\*</sup>, J.E.T. Channell<sup>b</sup>, J.S. Stoner<sup>c</sup>

<sup>a</sup> Laboratoire des Sciences du Climat et de l'Environnement, CEA-CNRS-UVSQ, domaine du CNRS, 91198 Gif-sur-Yvette, France

<sup>b</sup> Department of Geological Sciences, University of Florida, PO Box 112120, 241 Williamson Hall, Gainesville, FL 32611, USA

<sup>c</sup> College of Oceanic and Atmospheric Sciences (COAS), Oregon State University, 104 COAS Administration Building, Corvallis, OR 97331-5503, USA

## ARTICLE INFO

### Article history:

Received 16 February 2015

Received in revised form 21 July 2015

Accepted 27 July 2015

Available online 13 August 2015

Editor: B. Buffett

### Keywords:

paleomagnetism

marine

current

sediment

record

paleointensity

## ABSTRACT

Integrated Ocean Drilling Program (IODP) Expedition 303 to the North Atlantic in 2004 recovered a 175-m Quaternary sedimentary section at IODP Site U1307, located on the northern part of the Eirik Drift, south of Greenland. The seafloor at Site U1307, at 2575 m water depth, is situated within the water-depth range of the present-day main axis of the Western Boundary Under Current (WBUC) but lies on the NW side of the drift crest and is partly shielded from it. The uppermost 120 meters of sediment sequence were sampled with u-channels along a composite section which combines the two holes drilled at this site. An age model was obtained by identification of polarity reversals back to the Reunion Subchron (~2.1 Ma) and then refined in the 0–1.5 Ma interval by correlation of the relative paleointensity (RPI) record to the PISO paleointensity stack. The Site U1307 relative paleointensity (RPI) record is compared with the PISO and EPAPIS (Pacific) stacks, neighboring IODP sites from Eirik Drift (Sites U1305 and U1306), and with the Ocean Drilling Program (ODP) Site 984 record that extends beyond PISO. Magnetite grain-size and concentration proxies are compared to Sites U1305 and U1306 records, in the context of the past evolution of the WBUC.

© 2015 Elsevier B.V. All rights reserved.

## 1. Introduction

Expedition 303 of the Integrated Ocean Drilling Program (IODP) took place during September to November 2004 in the North Atlantic Ocean with the aim to explore Quaternary millennial-scale climatic and hydrographic change, as well as to obtain records of past geomagnetic field variations. IODP Site U1307 (58°30.3'N, 46°24.0'W) is located NE of the crest of the main ridge of the Eirik Drift, off southern Greenland (Fig. 1), 53 km NW of Site U1306 and 168 km NE of Site U1305, also drilled during IODP Expedition 303. Like other sites in this area, Site U1307 receives detritus from Greenland, in response to ice-sheet advances and retreats, and also material transported by the Western Boundary Under-Current (WBUC), also referred to as the Deep Western Boundary Current (DWBC). This current flows in this area at a depth between 1900 and 3000 m at the present time. It shoaled and slowed during glacial times, with reduced North Atlantic Deep Water production and increased advection of southern ocean waters (Hall and Becker, 2007; Hillaire-Marcel et al., 2011). The seafloor at Site U1307 is thus within the depth range of the present-day main

axis of the WBUC. This current is largely fed by Denmark Strait Overflow Water (DSOW), and by Iceland–Scotland Overflow Water (ISOW) that forms North-East Atlantic Deep Water (NEADW) (Hunter et al., 2007). DSOW and NEADW converge to form the WBUC (Fig. 1). After flowing over Eirik Drift, the WBUC joins the DSO (Davis Strait Overflow Water) and the LSW (Labrador Sea Water) to produce North Atlantic Deep Water (NADW). The Eirik Drift also receives, to lesser extent, material from the Labrador Sea associated with Laurentide Ice Sheet (LIS) dynamics (Stoner et al., 1995a; Stanford et al., 2006, 2011; Evans et al., 2007; Colville et al., 2011).

Two holes were drilled at Site U1307 to a depth below seafloor of ~160 m using the Advanced Piston Corer (APC) with non-magnetic core barrels that limit magnetic overprinting during coring (Lund et al., 2003). The sediments are dominated by terrigenous materials comprising clay minerals, quartz and detrital carbonate, with a biogenic component. The most common lithologies are dark gray to very dark gray silty clays with nannofossils (Shipboard Scientific Party, 2006). A stratigraphic composite section was constructed shipboard, largely based on magnetic susceptibility data collected with the susceptibility core logger (Shipboard Scientific Party, 2006). Correlation was unambiguous down to ~76.4 meters composite depth (mcd). Hole U1307B was pre-

\* Corresponding author.

E-mail address: alain.mazaud@lscce.ipsl.fr (A. Mazaud).

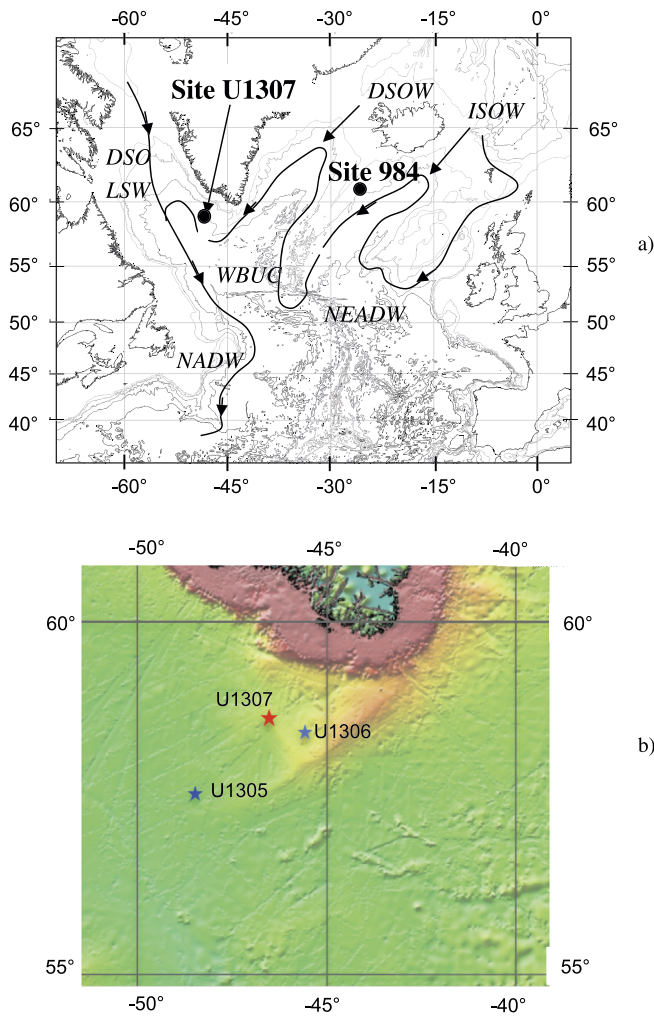


**Fig. 1.** a) Location of IODP Site U1307 on Eirik Drift in the North Atlantic Ocean, south of Greenland, and locations for IODP Sites U1305 and U1306, and ODP Site 984. Principal ocean currents are indicated by arrows: Denmark Strait Overflow Water (DSOW), Iceland–Scotland Overflow Water (ISOW), North East Atlantic Deep Water (NEADW), Western Boundary Under-Current (WBUC), Davis Strait Overflow Water (DSO), North Atlantic Deep Water (NADW). Adapted from [Hillaire-Marcel et al. \(2011\)](#). b) Bathymetry and location of IODP Sites U1305, U1306, and U1307 in the vicinity of Eirik Drift (from [Smith and Sandwell, 1997](#)).

ferred in the 56.5–66.5 mcd interval, because drilling disturbance at 56.5 mcd in Hole U1307A prevented reliable correlation to Hole U1307B. Correlation is tenuous at  $\sim 76.4$  mcd and  $\sim 104.7$  mcd, but generally satisfactory between 76.4 mcd and 104.7 mcd. A basal age of  $\sim 3.5$  Ma was estimated from preliminary shipboard stratigraphy ([Shipboard Scientific Party, 2006](#)). Paleomagnetic measurements were conducted shipboard on archive-half core sections using the shipboard pass-through cryogenic magnetometer, using a down-core measurement spacing of 15 cm. Aboard ship, the natural remanent magnetization (NRM) intensities and directions were measured on half-core sections before any demagnetization was performed, and then after alternating field (AF) demagnetization that was restricted to peak fields of 10 mT, or occasionally 20 mT, to ensure that archive halves remained useful for shore-based high-resolution u-channel measurements.

NRM intensities before demagnetization ranged from  $\sim 10^{-1}$  A/m to more than 1 A/m. After AF demagnetization at peak fields of 10–20 mT, NRM intensities drop to  $\sim 10^{-1}$  A/m. Despite limited AF demagnetization, shipboard measurements enabled clear identification of the Brunhes, Matuyama and Gauss polarity chrons. Within the Matuyama Chron, the Jaramillo, Olduvai, and Reunion

Subchrons are clearly recognized. Within the Gauss Chron, the Kaena and Mammoth Subchrons are also tentatively recognized, with the base of the section corresponding to the top of the Gilbert Chron ([Shipboard Scientific Party, 2006](#)). The mean sedimentation rate at Site U1307 calculated using shipboard magnetostatigraphic (and biostratigraphic) markers was estimated to be  $\sim 5$  cm/kyr.

## 2. Sampling and laboratory methods

The Site U1307 composite section was sampled with u-channels at the IODP core repository in Bremen (Germany) down to a depth of 120 mcd, which corresponds to an age of  $\sim 2.2$  Ma according to shipboard stratigraphy. Sediment hardness and compaction prevented sampling below this depth. Natural remanent magnetization (NRM) was measured at 1-cm intervals for each u-channel sample at the LSCE paleomagnetic laboratory at Gif-sur-Yvette (France), using small-diameter pass-through cryogenic magnetometers specifically designed for u-channel measurements ([Weeks et al., 1993](#)). These instruments allow a spatial resolution of  $\sim 4.5$  cm, that is an improvement in resolution compared to the shipboard magnetometer on board the R/V *Joides Resolution*. Stepwise AF demagnetization of the NRM was conducted up to peak fields of 80 mT using the 3-axis AF demagnetization system placed in-line with the magnetometer sample track. Component magnetization directions and maximum angular deviation (MAD) values, which monitor the quality of the characteristic magnetization components, were then determined for the 20–60 mT demagnetization intervals, by using the standard “principal component” method of [Kirschvink \(1980\)](#) through Excel spreadsheet software ([Mazaud, 2005](#)). Component declinations were adjusted according to the shipboard “Tensor Multishot” orientation measurements, where available, or by uniform rotation of each individual core, such that the core mean declination for intervals outside polarity transitions equals  $0^\circ$  or  $180^\circ$ . The tensor tool consists of a three-component fluxgate magnetometer and a three-component accelerometer rigidly attached to the core barrel to record the azimuth and dip of each core ([Shipboard Scientific Party, 2006](#)).

After measurement of the NRM, low-field volume magnetic susceptibility ( $\kappa$ ), anhysteretic remanent magnetization (ARM), and isothermal remanent magnetization (IRM) were measured at 1-cm intervals for each u-channel sample. Susceptibility is controlled by the concentration of ferromagnetic (*s.l.*) minerals in these sediments. Measurements of low-field bulk susceptibility ( $\kappa$ ) were performed at Gif-sur-Yvette using a small diameter (4 cm) Bartington instrument loop sensor mounted in line with a track system designed for u-channels. ARM and IRM are remanent magnetizations, controlled by the concentration of the ferromagnetic (*s.l.*) fraction. ARM is more sensitive to small magnetic grains, with sizes around 0.1–5  $\mu\text{m}$ , while IRM is sensitive to a wider spectrum of grain sizes, up to several tens of microns ([Maher, 1988; Dunlop and Özdemir, 1997](#)). ARM was acquired along the axis of the u-channel using a 100 mT AF field and a 50  $\mu\text{T}$  direct current (DC) bias field. Anhysteretic susceptibility ( $\kappa_{\text{ARM}}$ ) was then determined by normalizing ARM values by the DC field value ([King et al., 1983](#)). The ARM was also demagnetized, using the same steps as those used for the NRM. An IRM was acquired in 6 steps up to 1 T using a 2G Enterprises pulse IRM solenoid. The  $\text{IRM}_{1\text{T}}$  was stepwise demagnetized. Then, after re-acquisition of an IRM at 1 T, a backfield of 0.3 T was applied to calculate the S-ratio where  $S_{-0.3\text{T}} = -\text{IRM}_{-0.3\text{T}}/\text{IRM}_{1\text{T}}$  ([King and Channell, 1991](#)), and  $S_{-0.3\text{T}}$  provides a measure of the magnetic coercivity, which, in turn, provides information on magnetic mineralogy.

Magnetic hysteresis parameters were measured using a Princeton Measurements Corp. vibrating sample magnetometer (VSM) at the University of Florida on samples obtained on cleaning each

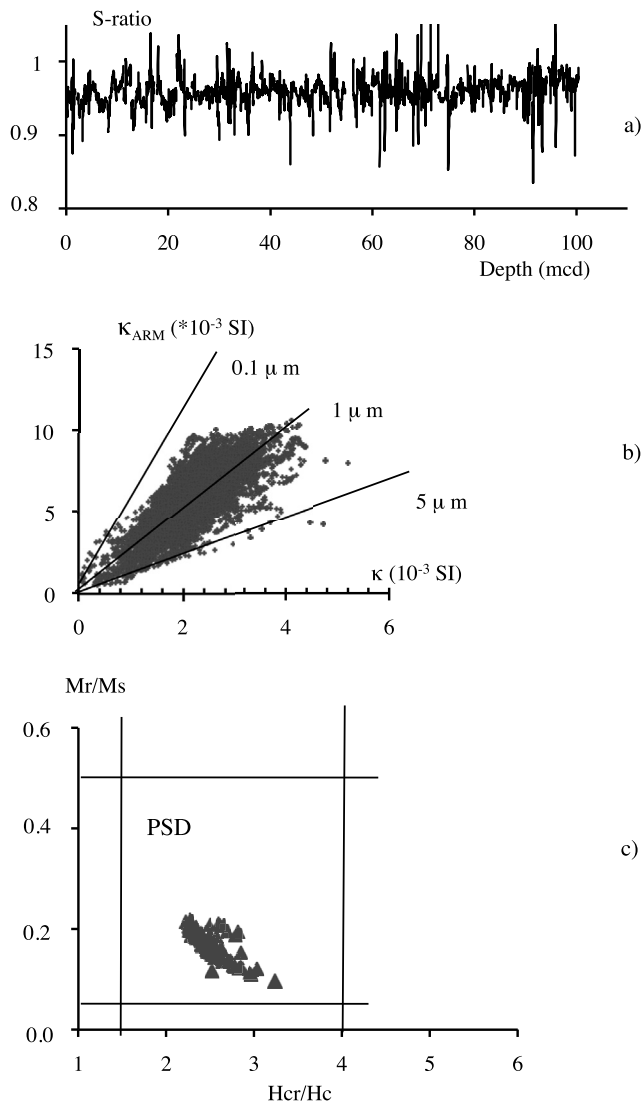


**Fig. 2.** a) S-ratio plotted versus meters composite depth (mcd). b)  $\kappa_{\text{ARM}}$  versus  $\kappa$  diagram with a 30 mT peak field demagnetization applied to the ARM (see Channell et al., 2014). Lines indicate locus of magnetite grain sizes of 0.1, 1, and 5  $\mu\text{m}$ , as estimated by King et al. (1983). c) Hysteresis ratios for single samples associated with each u-channel sample from the composite section, plotted on a Day et al. (1977) diagram (MD: multi-domain grains, PSD: pseudo-single domain, SD: single domain).

individual u-channel during sampling. The hysteresis parameters were used to assess magnetic mineralogy and grain size.

### 3. Magnetic mineralogy

Previous investigations of cores taken on Eirik Drift indicate a magnetic mineralogy dominated by (titano)magnetite, with variable grain size primarily in the pseudo-single domain (PSD) range (Stoner et al., 1995a, 1995b, 1996; Evans et al., 2007; Mazaud et al., 2012; Kawamura et al., 2012; Channell et al., 2014). Values of the S-ratio at Site U1307 are close to unity (Fig. 2a), indicating that low coercivity magnetic minerals (e.g. magnetite) dominate the magnetic mineralogy. The  $\kappa_{\text{ARM}}$  versus  $\kappa$  diagram shows an elongated distribution emanating from the origin of the graph, with limited dispersion in slope indicate uniformity in magnetite grain size (Fig. 2b). According to the calibration of King et al. (1983), the  $\kappa_{\text{ARM}}$  versus  $\kappa$  diagram implies a magnetite grain size in the 1–5  $\mu\text{m}$  range (Fig. 2b). These estimates are consistent with magnetite grain size based on the

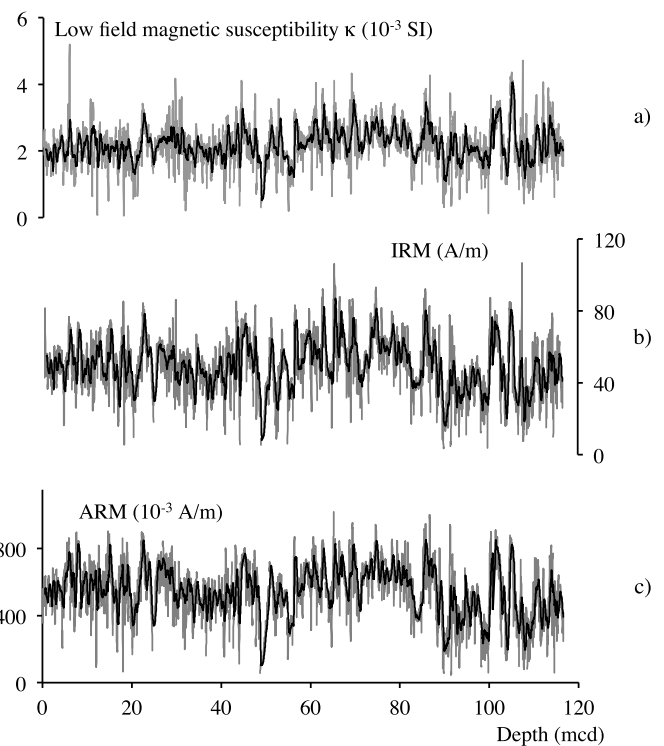


**Fig. 3.** Records of three bulk magnetic parameters: volume susceptibility ( $\kappa$ ), anhysteretic remanent magnetization (ARM) and isothermal remanent magnetization (IRM) versus meters composite depth (mcd). Gray curve, unsmoothed record; dark curve, after smoothing with a 50-cm sliding window.

“Day” plot (Day et al., 1977) of magnetic hysteresis parameters, where hysteresis ratios lie in the pseudo-single domain (PSD) field and are distributed along the magnetite grain-size mixing line (Fig. 2c).

Values of three bulk magnetic parameters ( $\kappa$ , ARM and IRM) along the Site U1307 composite section (Fig. 3) are within an order of magnitude indicating that the sediments adhere to generally accepted suitability criteria for the determination of relative paleointensities (King et al., 1983; Tauxe, 1993). The largest fluctuations are observed at depths below 80 mcd (Fig. 3). A close similarity between  $\kappa$  and IRM indicates negligible contribution of paramagnetic minerals to the susceptibility signal. Overall, Site U1307 magnetic properties resemble those from Site U1305 (Mazaud et al., 2012) and Site U1306 (Channell et al., 2014), indicating a magnetite-dominated mineralogy with grain sizes in the PSD field.

### 4. Paleomagnetic record of the past 2.2 millions years

AF demagnetization of the NRM along the composite section indicates a stable characteristic magnetization direction obtained after demagnetization at peak fields greater than 20 mT. Typical orthogonal projections of demagnetization data indicate well-defined magnetization components with the exemption of an interval represented by the sample from 89.85 mcd (Supplementary Fig. 1). The u-channel record of component magnetization directions (declination and inclination) calculated for the 20–60 mT peak field demagnetization interval are shown in Fig. 4a–c, together with MAD values. Component inclination varies close to the expected value (72.5°) for a geocentric axial dipole field at the site latitude, for both polarities.

NRM intensity depends on the strength of the geomagnetic field that oriented the magnetic grains at or shortly after deposition, but also on the mineralogy, concentration and size of the magnetic

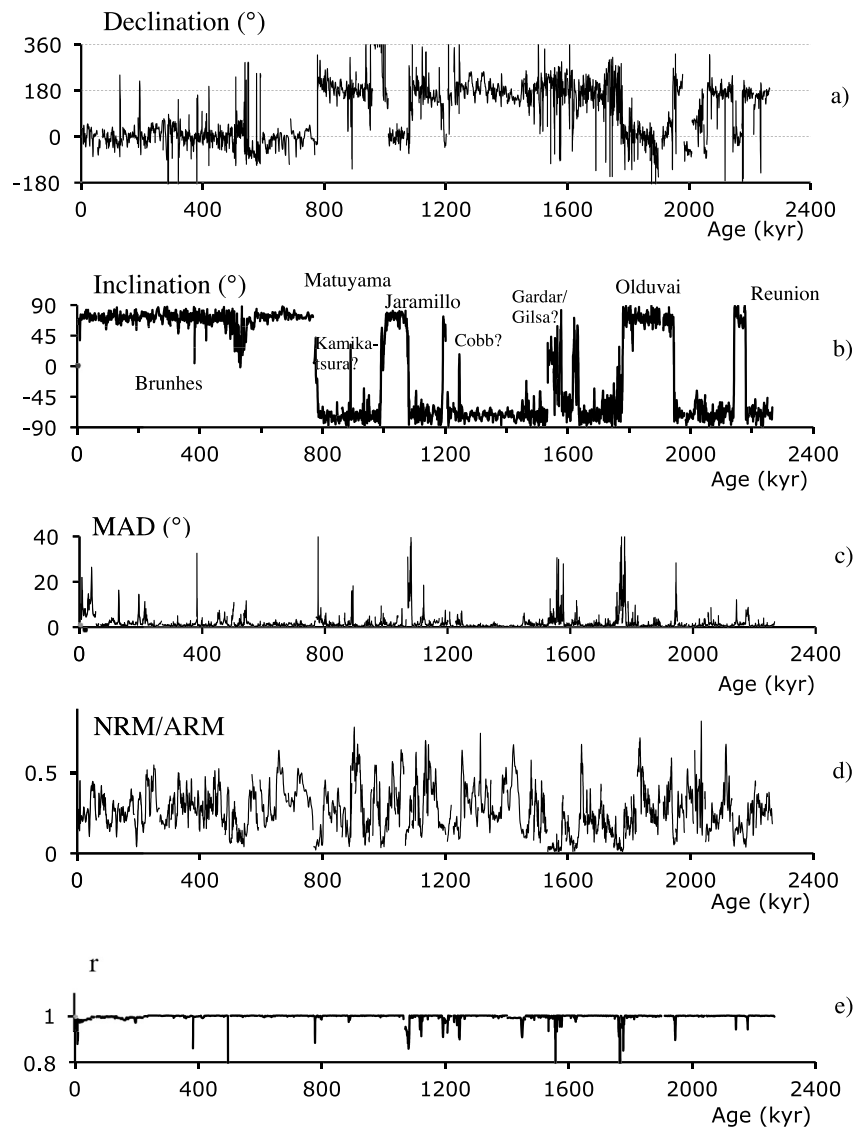


**Fig. 4.** Natural remanent magnetization (NRM) component declinations (a), inclinations (b), and maximum angular deviation (MAD) values (c), plotted versus age. d) Relative paleointensity proxies obtained from slopes of NRM versus ARM for the 20–60 mT peak field demagnetization interval. e) Regression factors (linear correlation coefficients:  $r$ ) obtained for the NRM/ARM slopes (see text).

grains, along with the characteristics of the non-magnetic matrix that may also influence alignment efficiency. Studies of past geomagnetic field intensity changes, or relative paleointensity (RPI), should be carried out on sediments in which magnetite is the only magnetic mineral, with small variations in magnetite grain size and concentration (King et al., 1983; Tauxe, 1993). ARM, which is sensitive to magnetite grains that carry NRM, is commonly used as a normalizer for the NRM intensity, and the NRM/ARM ratio is used as a proxy for RPI (Banerjee and Mellema, 1974; Levi and Banerjee, 1976; King et al., 1983; Tauxe, 1993). Here, we determine the RPI proxy (Fig. 4d) by calculating the NRM–ARM regression (slope) in the 20–50 mT peak AF interval (Channell et al., 2002). The linear correlation coefficient ( $r$ ) is used to indicate the quality of definition of the NRM/ARM slopes (Fig. 4e). At Site U1307, correlation coefficients close to unity (around 0.99) predominate, with values lower than 0.95 principally obtained during polarity reversals and apparent geomagnetic excursions. The RPI record reveals marked fluctuations, with, as expected, broad minima at the time of polarity transitions. RPI proxies obtained by normalizing NRM by IRM, or  $\kappa$ , do not differ markedly from the record obtained using ARM (Fig. 5), thereby adding confidence to

the RPI record. The different normalized remanence values, compared using scatter plots, also indicate consistency among the RPI proxies (Supplementary Fig. 2).

The age model was determined by identifying polarity reversals at the Matuyama–Brunhes boundary and the boundaries of the Jaramillo, Olduvai and Reunion Subchrons, consistent with identifications based on shipboard measurements (Channell et al., 2006), using the generally accepted ages for these polarity reversals (Lourens et al., 2004). In the 0–1.5 Ma interval, the age model was refined by correlation of the Site U1307 RPI signal to the PISO-1500 stack (Channell et al., 2009). A total of 21 tie-points were used to match the RPI signal to PISO, assuming uniform sedimentation rates between tie-points (Fig. 5b, Supplemental Table 1). The PISO-1500 RPI stack (Channell et al., 2009) was constructed by “tandem” correlation of the RPI and  $\delta^{18}\text{O}$  records, from 12 mainly North Atlantic sites, to RPI and  $\delta^{18}\text{O}$  records from the thirteenth site (North Atlantic IODP Site U1308). The Site U1308 age model, and the PISO-1500 age model back to 1.5 Ma, were based on correlation of the Site U1308 benthic  $\delta^{18}\text{O}$  record (Hodell and Curtis, 2008) to LR04, the global  $\delta^{18}\text{O}$  stack (Lisiecki and Raymo, 2005).

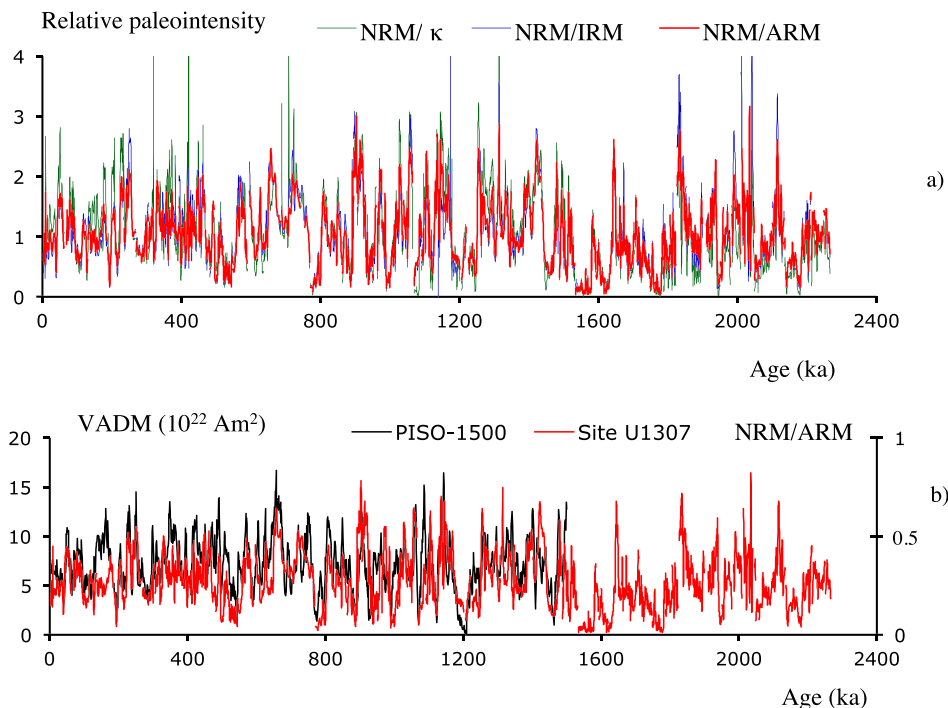


**Fig. 5.** a) Relative paleointensity proxies obtained using susceptibility ( $\kappa$ ), anhysteretic remanent magnetization (ARM) and isothermal remanent magnetization (IRM) as normalizers of the natural remanent magnetization (NRM). b) Comparison between the PISO-1500 stack and Site U1307 relative paleointensity (NRM/ARM) record.

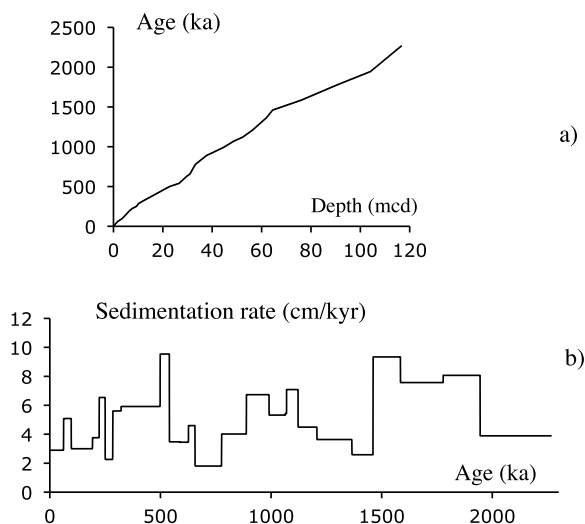


**Fig. 6.** a) Age versus depth model for Site U1307. b) Corresponding sedimentation rates.

Beyond 1.5 Ma, the Site U1307 age model (Fig. 6, Supplemental Table 1) relies entirely on the position of the boundaries of the Olduvai and Reunion Subchrons (Fig. 4b), and current accepted ages for these subchron boundaries (Lourens et al., 2004). The Site U1307 age model indicates that the 120 m studied sequence covers the past 2.26 ka, which corresponds to almost the entire Quaternary, with a mean sedimentation rate of  $\sim 5.5$  cm/kyr (Fig. 6).

Confidence in Site U1307 age model, for the last 1.5 Myr, based on the satisfactory correlation to the PISO stack, is enhanced by the results of spectral analyses of the RPI record, and the normalizer (ARM) used to acquire it. Spectral analyses were carried out using an autocorrelation power spectrum algorithm often used for time series analyses in paleoclimate studies, which includes a red noise confidence level calculation (Pestiaux and Berger, 1982, 1984). The power spectrum for ARM intensity indicates a small peak at a

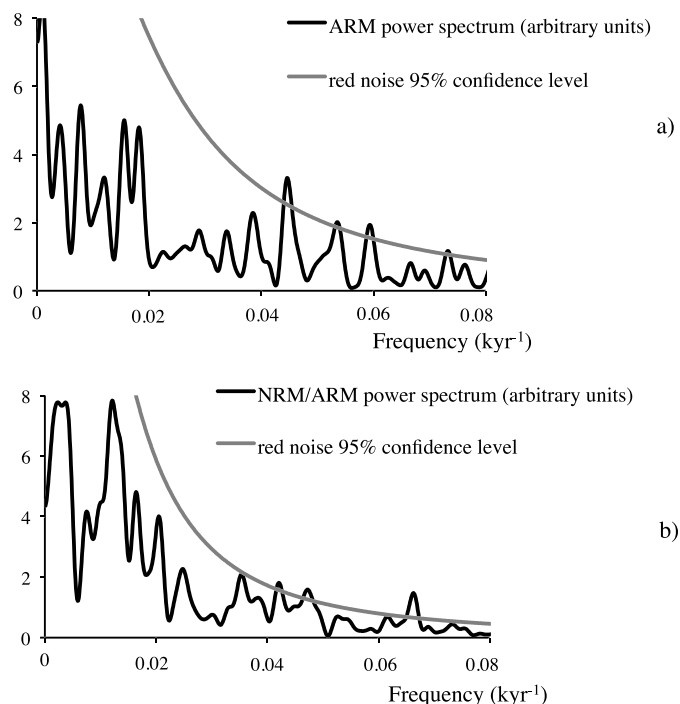


**Fig. 7.** a) Spectral analysis of the Site U1307 anhysteretic remanent magnetization (ARM) record. b) Spectral analysis of Site U1307 relative paleointensity (RPI) proxy based on NRM/ARM slopes.

period of  $\sim 22$  kyr ( $0.045 \text{ kyr}^{-1}$ ) that is visible above the 95% confidence level (Fig. 7a). Although not seen when using the REDFIT program (Schulz and Mudelsee, 2002), the presence of apparent precessional power in ARM intensity could indicate an influence of precession in the concentration of detrital magnetite. This  $\sim 22$ -kyr power does not appear in the RPI signal obtained from NRM/ARM slopes (Fig. 7b). This implies that the normalization procedure has

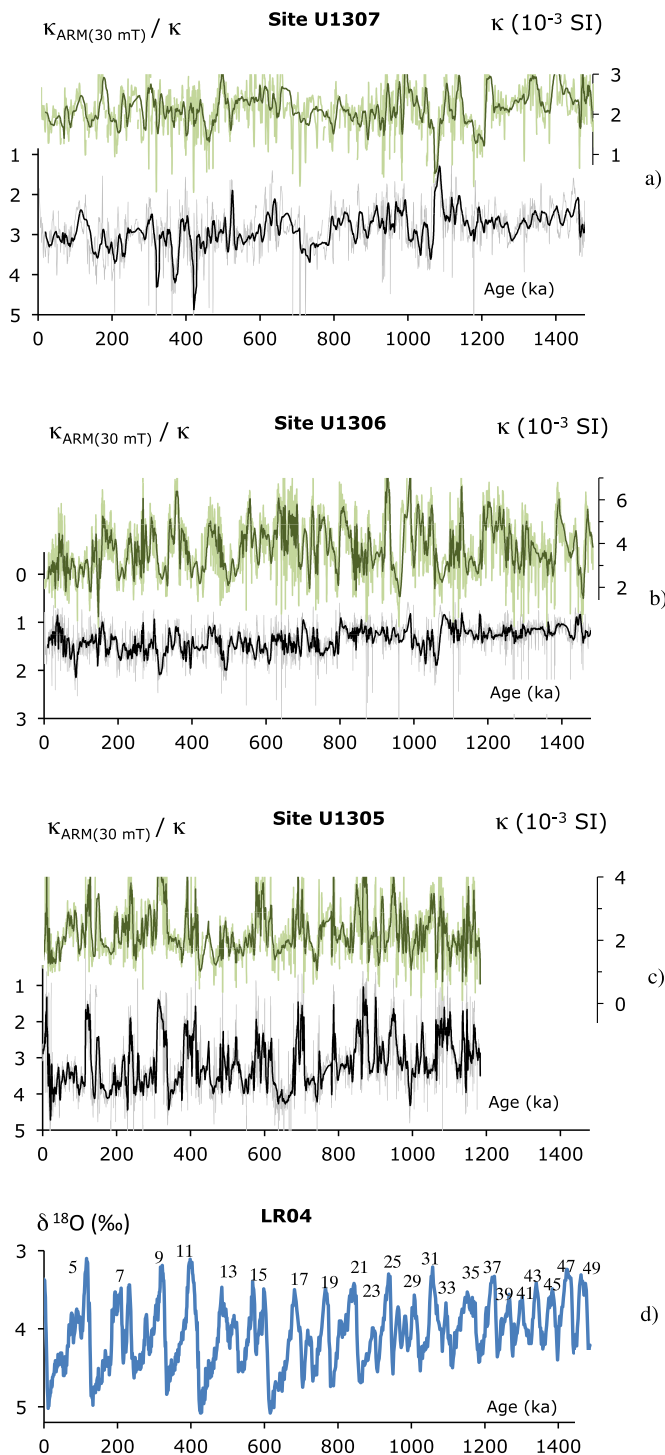


**Fig. 8.** a) Anhyseretic remanence divided by volume susceptibility ( $\kappa_{\text{ARM}}/\kappa$ ) and volume susceptibility ( $\kappa$ ) records obtained at Site U1307. b) Site U1306. c) Site U1305. d) Oxygen isotopic stack LR04 (Lisiecki and Raymo, 2005) with labeled interglacial marine isotopic stages.

removed most of the climatic and environmental influences in the RPI signal.

## 5. Discussion

Concentration of magnetic parameters have been used to trace transport of magnetite grains by bottom currents in the North Atlantic (Kissel et al., 1999, 2009). The ratio  $\kappa_{\text{ARM}}/\kappa$ , the anhyseretic susceptibility ( $\kappa_{\text{ARM}}$ ) divided by the volume susceptibility ( $\kappa$ ), or

ARM/ $\kappa$ , have been used as a proxy for magnetite grain-size variations (e.g., King et al., 1983; Maher, 1988; Verosub and Roberts, 1995; Tauxe, 1993; Dunlop and Özdemir, 1997). Low values of this ratio indicate large magnetite grains, while high values correspond to small grains. It has been used in the North Atlantic to trace the deep-water circulation changes, as well as influxes of detritus from south Greenland into the Labrador basin at the deglaciations (Stoner et al., 1995a, 1996; Evans et al., 2007; Stanford et al., 2006; Mazaud et al., 2012; Channell et al., 2014).

The Site U1307 low-field susceptibility signal ( $\kappa$ ), which traces the concentration of magnetite in these sediments, exhibits variations that are muted relative to variations observed at Site U1306 and Site U1305 (Fig. 8). Susceptibility variations at Site U1306 contrast with those at Site U1305 reflecting the enhanced detrital deposition in glacial and interglacial isotopic stages at Site U1306 and Site U1305, respectively (Channell et al., 2014). Site U1307 is located at slightly greater water depth (2575 m) than Site U1306 (2273 m), but appreciably shallower than Site U1305 (3460 m). As expected, the susceptibility pattern at Site U1307 is more similar to that at Site U1306 than that at Site U1305, being influenced by similar modes of detrital delivery. The mean sedimentation rate at Site U1307 is approximately half that at Site U1306 (Channell et al., 2014). This is consistent with a reduced input from the WBUC, reflecting the position of Site U1307 on the lee (NW) side of the drift, with Site U1306 closer to the drift crest (Fig. 1b). As for Site U1306,  $\kappa_{\text{ARM}}/\kappa$  values obtained at Site U1307 document limited variations, with a slow trend towards a grain size decrease during the past 1.5 Ma (Fig. 8). The difference in values of  $\kappa_{\text{ARM}}/\kappa$  for Site U1307 and Site U1306 (Fig. 8) may partially reflect differences in the acquisition of ARM in the Gif-sur-Yvette and Florida laboratories. Unlike Site U1307 and U1306, the  $\kappa_{\text{ARM}}/\kappa$  values at Site U1305 indicate markedly larger magnetite grain size during the interglacial isotopic stages (Fig. 8) during enhanced detrital transport to the site by the WBUC. Because of water depth and location, Site U1307 and Site U1306 were not influenced to the same extent as Site U1305 by past variations of the WBUC.

The Site U1307 RPI record resembles the PISO-1500 paleointensity stack (Channell et al., 2009) for the past 1500 ka (Fig. 5b). This similarity implies that the Site U1307 RPI record is a useful representation of past variations of the intensity of the Earth's axial dipole field. Some differences are observed between the Site U1307 RPI record and PISO-1500 stack, in particular around 130–180 ka, ~510 ka and 1460–1500 ka (Fig. 5b). The Site U1307 RPI record closely resembles the Site U1306 record for the 0–1500 ka interval (Fig. 9a) and satisfactory agreement is also observed with most of the Site U1305 record although correlation is poor in the 100–150 ka and 450–550 ka intervals, and at ~300 ka (Fig. 9b). The marked intensity low at ~190 ka appears at a slightly younger age in the Site U1305 record than in the Site U1307 record (Fig. 9b), providing one prominent example of differences in the age models.

At older ages >1.5 Ma, we have compared the Site U1307 RPI record to records from ODP Sites 984, also obtained in the North Atlantic (Channell et al., 2002), and to the EPAPIS stack from the equatorial Pacific that extends back to 3 Ma (Yamazaki and Oda, 2005). The independent age models give satisfactory fit among the different records for 1.8–2.2 Ma, although not in the 1.5–1.8 Ma interval where all three records differ (Fig. 9c). High MAD values are observed for Site U1307 in the 1.5–1.8 Ma interval (Fig. 4c) due to poorly defined magnetization components reflected in orthogonal projections of demagnetization data from this interval (Supplementary Fig. 1). The broad low in RPI in the 1530–1580 ka interval at Site U1307 is anomalous relative to EPAPIS and Site 984 (Fig. 9c) due to poorly defined magnetization components in this interval. The RPI low observed between 1550–1580 ka in the Site 984 record coincides with a directional magnetic excursion

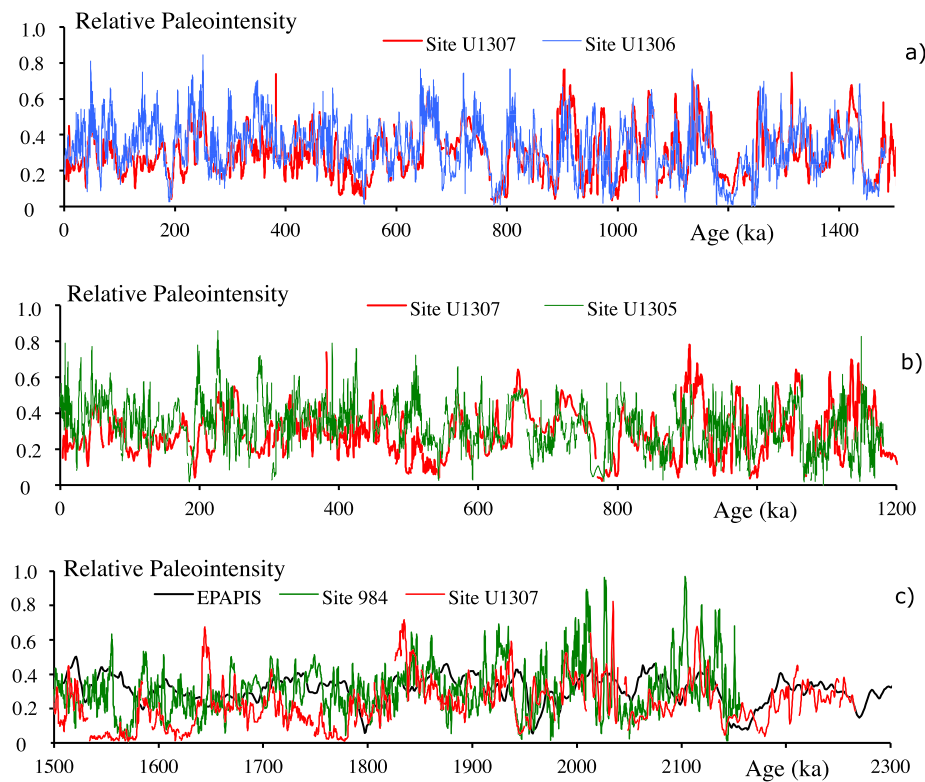


**Fig. 9.** a) Comparison of relative paleointensity (RPI) records from Sites U1307 and U1306 for the 0–1500 ka interval. b) Comparison of RPI records for Sites U1307 and U1305 for the 0–1200 ka interval. c) Comparison of Site U1307 RPI record with the EPAPIS stack (Yamazaki and Oda, 2005), and the RPI record from ODP Sites 984 (Channell et al., 2002), for the 1500–2300 ka interval. All records are placed on their independent (published) age models.

sion (the Gilsa excursion) recorded at this site (Channell et al., 2002). The EPAPIS stack indicates a more subdued minimum at ~1590 ka. These differences cannot be entirely attributed to uncertainties in the Site U1307 age model that is, however, not constrained between the end of the PISO stack (at 1.5 Ma) and the top of the Olduvai Subchron at 1.7 Ma. Overall, the compared RPI records are similar, particularly since 1.5 Myr, with some offsets that suggest chronological mismatches (Fig. 9). In view of the contrasting sedimentation rates and glacial/interglacial sedimentation rate patterns at the Eirik Drift IODP sites (Mazaud et al., 2012; Channell et al., 2014), results indicate that Site U1307 provides a long (2.2 Myr) record of past field intensity, that can be used for stratigraphic correlation.

## Acknowledgements

Laboratory investigations were funded by the French Commissariat à l’Energie Atomique (CEA) and the Centre National de la Recherche Scientifique (CNRS), and by US National Science Foundation Grants 0850413 and 1014506. Samples were provided by the Integrated Ocean Drilling Program (IODP) and we thank the crew and scientists aboard the RV *Joides Resolution* during Expedition 303, the IODP staff, and the curatorial staff of the Bremen core repository. Participation in IODP Expedition 303/306 was funded by the Integrated Ocean Drilling Program. Data are available in Supplementary Table 2. This is LSCE contribution No. 5509.

## Appendix A. Supplementary material

Supplementary material related to this article can be found online at <http://dx.doi.org/10.1016/j.epsl.2015.07.059>.

## References

- Banerjee, S.K., Mellema, J.P., 1974. A new method for the determination of paleointensity from the ARM properties of rocks. *Earth Planet. Sci. Lett.* 23, 177–184.
- Channell, J.E.T., Kanamatsu, T., Sato, T., Stein, R., Alvarez Zarikian, C.A., Malone, M.J., Expedition 303/306 Scientists, 2006. In: *Proc. IODP, 303/306. Integrated Ocean Drilling Program Management International, Inc., College Station, TX.*
- Channell, J.E.T., Mazaud, A., Sullivan, P., Turner, S., Raymo, M.E., 2002. Geomagnetic excursions and paleointensities in the 0.9–2.15 Ma interval of the Matuyama chron at ODP Site 983 and 984 (Iceland Basin). *J. Geophys. Res.* 107, 2114. <http://dx.doi.org/10.1029/2001JB000491>.
- Channell, J.E.T., Wright, J.D., Mazaud, A., Stoner, J.S., 2014. Age through tandem correlation of Quaternary relative paleointensity (RPI) and oxygen isotope data at IODP Site U1306 (Eirik Drift, SW Greenland). *Quat. Sci. Rev.* 88, 135–146.
- Channell, J.E.T., Xuan, C., Hodell, D.A., 2009. Stacking paleointensity and oxygen isotope data for the last 1.5 Myr (PISO-1500). *Earth Planet. Sci. Lett.* 283, 14–23.
- Colville, E.J., Carlson, A.E., Beard, B.L., Hatfield, R.G., Stoner, J.S., Reyes, A.V., Ullman, D.J., 2011. Sr–Nd–Pb isotope evidence for ice-sheet presence on southern Greenland during the last interglacial. *Science* 333, 620–623.
- Day, R., Fuller, M., Schmidt, V.A., 1977. Hysteresis properties of titanomagnetites: grain-size and compositional dependence. *Phys. Earth Planet. Inter.* 13, 260–267.
- Dunlop, D., Özdemir, Ö., 1997. *Rock Magnetism: Fundamentals and Frontiers*. Cambridge University Press. 595 pp.
- Evans, H.F., Channell, J.E.T., Stoner, J.S., Hillaire-Marcel, C., Wright, J.D., Neitzke, L.C., Mountain, G.S., 2007. Paleointensity-assisted chronostratigraphy of detrital layers on the Eirik Drift (North Atlantic) since marine isotope stage 11. *Geochem. Geophys. Geosyst.* 8. <http://dx.doi.org/10.1029/2007GC111720>.
- Hall, I.R., Becker, J., 2007. Deep Western Boundary Current variability in the subtropical northwest Atlantic Ocean during marine isotope stages 12–10. *Geochem. Geophys. Geosyst.* 8, Q06013. <http://dx.doi.org/10.1029/2006GC001518>.
- Hillaire-Marcel, C., de Vernal, A., McKay, J.L., 2011. Foraminifera isotope study of the Pleistocene Labrador Sea, northwest North Atlantic (IODP Sites 1302/03 and 1305), with emphasis on paleoceanographical differences between its “inner” and “outer” basins. *Mar. Geol.* 279, 188–198.
- Hodell, D.A., Curtis, J.H., 2008. Oxygen and carbon isotopes of detrital carbonate in North Atlantic Heinrich Events. *Mar. Geol.* 256 (1–4), 30–35.
- Hunter, S., Wilkinson, D., Louarn, E., McCave, I.N., Rohling, E., Stow, D.A.V., Bacon, S., 2007. Deep western boundary current dynamics and associated sedimentation on the Eirik Drift, Southern Greenland Margin. *Deep Sea Res., Part 1* 54, 2036–2066.

- Kawamura, N., Ishikawa, N., Torii, M., 2012. Diagenetic alteration of magnetic minerals in Labrador Sea sediments (IODP Sites U1305, U1306, and U1307). *Geochem. Geophys. Geosyst.* 13 (8), Q08013. <http://dx.doi.org/10.1029/2012GC004213>.
- King, J.W., Banerjee, S.K., Marvin, J., 1983. A new rock-magnetic approach to selecting sediments for geomagnetic paleointensity studies: application to paleointensity for the last 4000 years. *J. Geophys. Res.* 88, 5911–5920.
- King, J.W., Channell, J.E.T., 1991. Sedimentary magnetism, environmental magnetism, and magnetostratigraphy. *Rev. Geophys. Suppl.*, 358–370.
- Kirschvink, J.L., 1980. The least squares lines and plane analysis of palaeomagnetic data. *Geophys. J. R. Astron. Soc.* 62, 699–718.
- Kissel, C., Laj, C., Labeyrie, L., Dokken, T., Voelker, A., Blamart, D., 1999. Rapid climatic variations during marine isotopic stage 3: magnetic analysis of North Atlantic sediments. *Earth Planet. Sci. Lett.* 171, 489–502.
- Kissel, C., Laj, C., Mudler, T., Wandres, C., Cremer, M., 2009. The magnetic fraction: a tracer of deep water circulation in the North Atlantic sediments. *Earth Planet. Sci. Lett.* 288, 444–454.
- Levi, S., Banerjee, S.K., 1976. On the possibility of obtaining relative paleointensities from lake sediments. *Earth Planet. Sci. Lett.* 29, 219–226.
- Lisiecki, L.E., Raymo, M.E., 2005. A Pliocene–Pleistocene stack of 57 globally distributed benthic  $\delta^{18}O$  records. *Paleoceanography* 20, PA1003. <http://dx.doi.org/10.1029/2004PA001071>.
- Lourens, L.J., Hilgen, F.J., Lasker, J., Shackleton, N.J., Wilson, D., 2004. The Neogene period. In: Gradstein, F.M., et al. (Eds.), *A Geologic Time Scale*. Cambridge University Press, pp. 409–440.
- Lund, S.P., Stoner, J.S., Mix, A.C., Tiedermann, R., Blum, P., 2003. The 202 Leg Shipboard Scientific Party, 2003. In: *Proceedings of the Ocean Drilling Program, Initial Reports*, vol. 202.
- Maher, B.A., 1988. Magnetic-properties of some synthetic sub-micron magnetites. *Geophys. J.* 94 (1), 83–96.
- Mazaud, A., 2005. User-friendly software for vector analysis of the magnetization of long sediment cores. *Geochem. Geophys. Geosyst.*, Q120006. <http://dx.doi.org/10.1029/2005GC001036>.
- Mazaud, A., Channell, J.E.T., Stoner, J.S., 2012. Relative paleointensity and environmental magnetism since 1.2 Ma at IODP site U1305 (Eirik Drift, NW Atlantic). *Earth Planet. Sci. Lett.* 357–358, 137–144. <http://dx.doi.org/10.1016/j.epsl.2012.09.037>.
- Pestiaux, P., Berger, A., 1982. Numerical methods in the search for periodicities and quasi-periodicities. *Inst. Astron. Geophys., Catholic Univ. Louvain-la-neuve*, p. 34.
- Pestiaux, P., Berger, A., 1984. An optimal approach to the spectral characteristics of the deep-sea climatic records. In: Reidel, D. (Ed.), *Milankovich and Climate, Part 1*. In: NATO ASI Ser. C, vol. 126. Kluwer, pp. 417–445.
- Schulz, M., Mudelsee, M., 2002. REDFIT: estimating red-noise spectra directly from unevenly spaced paleoclimatic time series. *Comput. Geosci.* 28, 421–426.
- Shipboard Scientific Party, 2006. Site U1305. In: Channell, J.E.T., Kanamatsu, T., Sato, T., Stein, R., Alvarez Zarikian, C.A., Malone, M.J., Expedition 303/306 Scientists (Eds.), *Proc. IODP, 303/306. Integrated Ocean Drilling Program Management International, Inc., College Station, TX*.
- Smith, W.H.F., Sandwell, D.T., 1997. Global seafloor topography from satellite altimetry and ship depth soundings. *Science* 277, 1957–1962.
- Stanford, J.D., Rohling, E.J., Bacon, S., Roberts, A.P., Grousset, F.E., Bolshaw, M., 2011. A new concept for the paleoceanographic evolution of Heinrich event 1 in the North Atlantic. *Quat. Sci. Rev.* 30, 1047–1066.
- Stanford, J.D., Rohling, E.J., Hunter, S.E., Roberts, A.P., Rasmussen, S.O., Bard, E., McManus, J., Fairbanks, R.G., 2006. Timing of mwp-1a and climate responses to meltwater injections. *Paleoceanography* 21, PA4103. <http://dx.doi.org/10.1029/2006PA001340>.
- Stoner, J.S., Channell, J.E.T., Hillaire-Marcel, C., 1995a. Magnetic properties of deep-sea sediments off southwest Greenland: evidence for major differences between the last two deglaciations. *Geology* 23, 241–244.
- Stoner, J.S., Channell, J.E.T., Hillaire-Marcel, C., 1995b. Late Pleistocene relative geomagnetic field paleointensity record from the deep Labrador Sea: regional and global correlations. *Earth Planet. Sci. Lett.* 134, 237–252.
- Stoner, J.S., Channell, J.E.T., Hillaire-Marcel, C., 1996. The magnetic signature of rapidly deposited detrital layers from the deep Labrador Sea: relationship to North Atlantic Heinrich Layers. *Paleoceanography* 11 (3), 309–325.
- Tauxe, L., 1993. Sedimentary records of relative paleointensity of the geomagnetic field: theory and practice. *Rev. Geophys.* 31, 319–354.
- Verosub, K.L., Roberts, A.P., 1995. Environmental magnetism: past, present and future. *J. Geophys. Res.* 100, 2175–2192.
- Weeks, R.J., Laj, C., Endignoux, L., Fuller, M., Roberts, A., Manganne, R., Blanchard, E., Goree, W., 1993. Improvements in long-core measurements techniques: applications in palaeomagnetism and palaeoceanography. *Geophys. J. Int.* 114, 651–662.
- Yamazaki, T., Oda, H., 2005. A geomagnetic paleointensity stack between 0.8 and 3.0 Ma from equatorial Pacific sediment cores. *Geochem. Geophys. Geosyst.*, Q11H20. <http://dx.doi.org/10.1029/2005GC001001>.